A long-lasting auroral spiral rotating around Saturn's pole

B. Palmaerts[1], Z. H. Yao[1,2], N. Sergis[3,4], R. L. Guo[1], D. Grodent[1], K. Dialynas[3], J.-C. Gérard[1], and D. G. Mitchell[5]

[1]Laboratoire de Physique Atmosphérique et Planétaire, Space sciences, Technologies and Astrophysics Research (STAR) Institute, Université de Liège, Liège, Belgium

[2]Key Laboratory of Earth and Planetary Physics, Institute of Geology and Geophysics, Chinese Academy of Sciences, Beijing, China

[3]Office of Space Research and Technology, Academy of Athens, Athens, Greece

[4]Institute of Astronomy, Astrophysics, Space Applications and Remote Sensing, National Observatory of Athens, Athens, Greece

[5]Applied Physics Laboratory, Johns Hopkins University, Laurel, MD, USA

Key Points:

- The main auroral emission forms a spiral observed during two consecutive days
- The spiral morphology is due to the presence of a hot plasma population in the magnetodisc
- The auroral spiral winds while the hot plasma bubble expands due to gradient and curvature drifts

Corresponding author: B. Palmaerts, b.palmaerts@uliege.be

This article has been accepted for publication and undergone full peer review but has not been through the copyediting, typesetting, pagination and proofreading process which may lead to differences between this version and the Version of Record. Please cite this article as doi: 10.1029/2020GL088810

Abstract

The main ultraviolet auroral emission at Saturn consists of multiple structures forming a discontinuous ring of emission around the poles, occasionally organized in a global spiral. We present continuous observation of an auroral spiral rotating at ~85% of rigid corotation during several hours. Simultaneously, energetic neutral atom (ENA) emissions revealed a hot magnetospheric plasma population located in the same local time sector as the ends of the rotating spiral. Following plasma theory, we propose that pressure gradients induced by the energized plasma distorted the magnetospheric current system, resulting in the spiral morphology of the aurora. The rotating hot plasma was several times re-energized in the dusk sector during at least two days, generating a long-lasting auroral spiral. The ultraviolet spiral, the ENA emissions and the ions revealed by this multi-instrument dataset are three signatures of a magnetosphere-ionosphere coupling current system and of the associated hot plasma population rotating around Saturn.

1 Introduction

Kronian ultraviolet (UV) aurora consists of many different structures associated with various magnetospheric processes such as magnetic reconnection, plasma injections and instabilities (see the review by *Grodent* [2015]). The so-called main auroral emission forms a discontinuous ring made up of multiple arc-like features and spots of various size around the poles. In the noon sector, the main emission can brighten and generate an elongated structure with an end moving polewards while drifting duskwards, forming a bifurcation of the main emission [*Radioti et al.*, 2011; *Badman et al.*, 2013]. These bifurcations have been interpreted as signatures of dayside magnetopause reconnection. On the opposite side of the magnetosphere, magnetotail reconnection, driven by solar wind compression or by mass loading, leads to a brightening and an expansion of the dawn portion of the main auroral emission (e.g. *Grodent et al.* [2005]; *Meredith et al.* [2014]; *Radioti et al.* [2016]; *Palmaerts et al.* [2018]). Such auroral dynamics in the dawn region are connected with plasma energization in the midnight-to-dawn sector and to the associated enhancements of the energetic neutral atom emissions [*Mitchell et al.*, 2009; *Dialynas et al.*, 2013].

Initial observations of Saturn's aurora with the Hubble Space Telescope (HST) have revealed that the main emission is occasionally organized in a spiral structure wrapping around the poles over more than 360° of longitude, with, in the dusk sector, one spiral end located at lower latitude than the other end [*Gérard et al.*, 2004]. During the Cassini approach of Saturn in 2004, the spiral morphology was again observed on HST auroral images, with the latitudinal discontinuity then located in the midnight-to-dawn sector [*Grodent et al.*, 2005]. More recently, an HST observing campaign of Saturn's aurora has shown new examples of the spiral shape of the main emission [*Lamy et al.*, 2018]. In all these observations, the spiral consistently showed the same structure with the latitude of the main emission decreasing with increasing local time.

All the published observations of the auroral spiral have been obtained using HST, enabling a continuous observing time limited to around 40 min. The long-term evolution of the spiral cannot be determined, which prevents accessing the global context necessary to interpret the spiral structure. Here we present Cassini auroral observations where the main emission forms a spiral which could be continuously tracked during ~7 hours with a sampling rate of ~21 minutes. We interpret remote and in-situ Cassini data to infer the underlying process causing the distortion of the main emission into a spiral structure.

2 Observations

2.1 Aurora

The Cassini spacecraft which orbited Saturn between 2004 and 2017 carried an Ultraviolet Imaging Spectrograph (UVIS), capable of capturing auroral light through a 64-pixel slit [*Esposito et al.*, 2004]. On August 17 (DOY 230) 2016, the northern polar region was scanned 29 times by the UVIS slit, providing 29 reconstructed images over a period of about 10 hours. During the observations, Cassini was approaching periapsis from 53° to 49° north and from 17 to 14.5 R_S.

The auroral images obtained in the UVIS Far-UV channel (111-191 nm) on day 230 at 18:09, 19:55, 22:25, and 23:51 UT are displayed at the top of Figure 1. They have been projected onto a polar map fixed in local time, following the procedure described in *Grodent et al.* [2011] and assuming an altitude of the auroral emissions peak at 1100 km above Saturn's 1-bar pressure level [*Gérard et al.*, 2009]. In Figure 1, the main auroral emission clearly forms a spiral wrapping around the pole, with the two ends overlapping over 70° of longitude. Like in previous observations [*Gérard et al.*, 2004; *Grodent et al.*, 2005; *Lamy et al.*, 2018], the latitude decreases with increasing local time. At 18:09 (Figure 1a), the

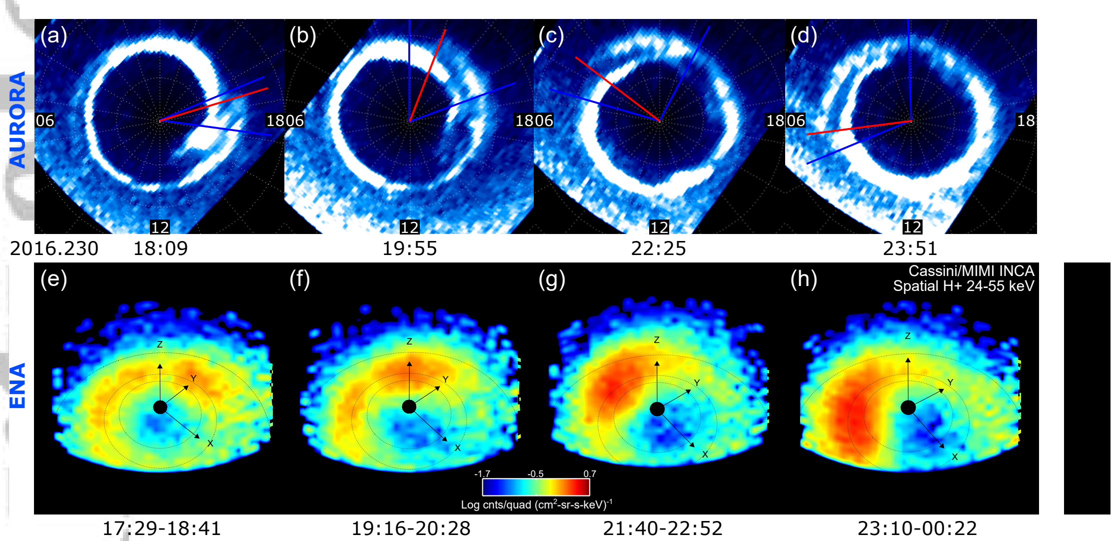

Figure 1. Top: Polar projections of four Cassini/UVIS images of the north FUV aurora, taken on 17 August 2016 (DOY 230). The direction of the Sun (12 LT) is towards the bottom. Bottom: Cassini/INCA images of 24-55 keV hydrogen ENA emissions acquired at the same time as the auroral images. The integration time of each frame is indicated below. The x-axis points towards the Sun, the y-axis points towards dusk and the z-axis is aligned with Saturn's rotation axis. The dotted circles indicate the orbits of Dione (6.2 R_S), Rhea (8.7 R_S) and Titan (20 R_S). On each UVIS projection, a red line indicates the approximate location of the low-latitude end of the auroral spiral and two blue lines bound the local time sector where the ENA cloud is observed on the INCA images.

local time of the overlapping region is located in the noon-to-dusk sector and reaches the midnight-to-dawn sector at the end of the sequence, 6.7 hours later (Figure 1d).

2.2 Energetic neutral atoms

Charge-exchange collisions between energetic ions and ambient neutral particles produce energetic neutral atoms (ENA) which travel in Saturn's magnetosphere in a straight line from their source. Hence, detecting ENA enables to remotely observe the energetic ion population from where they originate and the ENA emission intensity is related to the energetic ion intensities (e.g. *Dialynas et al.* [2013], *Mitchell et al.* [2016]). The Ion and Neutral Camera (INCA) on board Cassini, one of the three sensors of the Magnetosphere Imaging Instrument (MIMI, *Krimigis et al.* [2004]), detects the hydrogen ENAs between ~7 and 200 keV and the oxygen ENAs between ~32 and 200 keV through its 90° × 120°

field of view. The speed and the direction of the incoming neutrals are determined so that images of ENA emissions can be produced.

ENA imaging, in conjunction with in-situ ion observations, has allowed the observation of variations and asymmetries in Saturn's ring current [*Krimigis et al.*, 2007; *Khurana et al.*, 2009; *Dialynas et al.*, 2013, 2018; *Sergis et al.*, 2017, 2018]. These inhomogeneities in the ring current are partly due to inward injections of hot plasma energized on the nightside and drifting in the corotating direction around the planet, forming "blobs" in the ENA images [*Mitchell et al.*, 2005, 2009; *Carbary et al.*, 2008].

During the UVIS observations of the auroral spiral, INCA acquired images of ENA emissions in Saturn's magnetosphere. Four images of 24-55 keV hydrogen ENA are displayed in Figure 1e-h below the contemporaneous UVIS auroral image. For each ENA image, the emissions have been integrated over 72 min. While the ENA emissions were weak and diffuse in the duskside region before 17:10 UT, a small intensification appeared around dusk at the start of the UVIS sequence. This ENA cloud increased in intensity and extended in local time while rotating at constant radial distance towards dayside through midnight. The azimuthal expansion is due to gradient and curvature drifts of the particles within the energy width of the ENA channel and the radial distance occupied by the blob (e.g. *Brandt et al.* [2008]; *Mitchell et al.* [2009]), as discussed in Section 3. Simultaneous observations of the 55-90 keV proton ENAs and 90-170 keV oxygen ENAs (not displayed here) show a slight enhancement of emissions co-located with the strong hydrogen ENA emissions. These enhanced ENA emissions reveal the presence in Saturn's magnetodisc of a hot plasma population located at around 12 R_S from Saturn's center.

2.3 Angular velocity of the rotating auroral spiral and the contemporaneous energized magnetospheric plasma

The hot plasma population is located in the local time sector where the overlap region in the main auroral emission creates the spiral shape. The approximate local time position of the low-latitude end of the spiral and of the longitudinal boundaries of the hot plasma cloud (respectively indicated by a red and two blue lines in Figure 1a-d) are given in Figure 2. Linear fit of the displacement of the auroral spiral extremity indicates that the structure is rotating around the pole at an average rate of ∼1.9 LT/h, i.e. ∼85% of rigid corotation ($T_{rot} \simeq 10.79$ h in the northern hemisphere in 2016 [*Provan et al.*, 2019]).

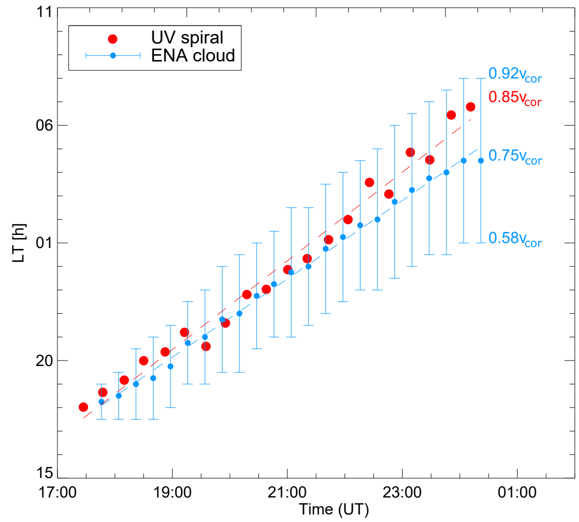

Figure 2. Local time position of the low-latitude end of the auroral spiral (red dots) and of the ENA cloud (blue bars and blue dots for the center). The dashed lines are linear fits of the red and blue dots. The velocities of the two edges and center of the ENA cloud and of the spiral low-latitude end are given on the right as a function of the rigid corotation velocity (v_{cor}).

The velocity of the leading edge of the hot plasma population is estimated to ~92% of the rigid corotation velocity (v_{cor}) while the trailing edge is limited at ~58% of v_{cor}, accounting for the expansion of the hot plasma bubble, the center of which is subcorotating at ~75% of v_{cor}. For comparison, Cassini in-situ plasma measurements have shown that the convection azimuthal velocity is typically ~70-80% of rigid corotation at ~6 R_S, where the inner boundary of the plasma population is located, and ~45-60% v_{cor} at ~18 R_S at the outer boundary, but large variations in azimuthal plasma velocities are observed (e.g. *Wilson et al.* [2017]; *Kane et al.* [2020]).

The coordinated rotation of the energized plasma around the planet and the auroral spiral around the pole strongly suggests that they are magnetically connected, similarly to other types of auroral structures [*Mitchell et al.*, 2009; *Lamy et al.*, 2013; *Radioti et al.*, 2013, 2019]. While particular auroral substructures can approach or even exceed corotation rate [*Radioti et al.*, 2015; *Nichols et al.*, 2014], global structures on closed field lines, like the main emission, rotate with an angular velocity close to ~70% of rigid corotation [*Grodent et al.*, 2005]. The auroral spiral depicted here rotates fast (~85% v_{cor}) for such a global structure.

3 Origin of the auroral spiral

During one of the first observations of the auroral spiral at Saturn, the monitoring of the solar wind by Cassini showed the arrival of an interplanetary shock which compressed the magnetosphere [*Grodent et al.*, 2005]. It was suggested by *Cowley et al.* [2005] that the auroral spiral resulted from a combination between the planetary rotation and the compression-induced reconnection of open flux in the tail lobes. The flux closure would then lead to a contraction of the main emission which, combined with the rotation, draws a spiral in which latitude decreases with increasing local time. In the absence of simultaneous in-situ measurements upstream of Saturn's magnetosphere, one cannot determine whether such a corotating interaction region (CIR) reached Saturn shortly before the observation of the auroral spiral reported here. However, a CIR arrival is generally followed by a contraction of the main emission [*Badman et al.*, 2005; *Grodent et al.*, 2005], which is not observed here. Moreover, an interplanetary shock does not seem to be required to develop a spiral since this auroral morphology has also been observed during undisturbed solar wind conditions [*Grodent et al.*, 2005]. We propose here another scenario involving the rotation of a hot plasma population around the planet, inspired from the ENA emission observations.

The presence of a hot plasma population creates a localized increase of the plasma pressure in the magnetodisc. The resulting pressure gradients at the boundaries of the plasma bubble drive a field-aligned current (FAC) system connecting the bubble and the ionosphere. According to the Vasyliūnas equation [*Vasyliunas*, 1970], the density of the ionospheric FACs is given by:

$$j_{\parallel} = \frac{B_{io}\hat{b}}{B_{eq}} \cdot \nabla V \times \nabla p \qquad (1)$$

where V is the flux tube volume per unit magnetic flux ($V = \int ds/B$), B is the magnetic field intensity, $\hat{b} = \mathbf{B}_{eq}/B_{eq}$ and subscripts *io* and *eq* refer to the ionosphere and the equatorial plane, respectively. Hence, since ∇V is mainly in the radial direction, the azimuthal pressure gradient at the leading (trailing) edge of the plasma bubble produces upward (downward) field-aligned currents. This FAC system is analogous to the region 2 current system coupling the Earth's ionosphere and the partial ring current (e.g. *Iijima and Potemra* [1978], *Brandt et al.* [2005], *Zheng et al.* [2008]). As a consequence, a layer of precipitating electrons is formed in addition to the layer associated with the main emission and located $\sim 10°$ in latitude polewards. This local time overlap of upward field-aligned currents in the ionosphere explains the two curtains of auroral emissions in the overlap region of the auroral spiral. It is however unclear how these two curtains connect to form a continuous spiral.

The Cassini 11 magnetic field model [*Dougherty et al.*, 2018] combined with a ring current model [*Bunce et al.*, 2007] connects the latitude range where the two curtains of emissions are found (~70-78°) to the equatorial region hosting the hot plasma population (6-17 R_S). The energetic protons producing the ENA emissions displayed in Figure 1 represent the main contribution to the pressure distribution and consequently to the pressure gradients (e.g. *Sergis et al.* [2017]), but ions at other energies and of other species could also moderately contribute.

Unlike at Earth where transient energized plasma populations develop in the nightside and are relatively fixed in local time, in the rotation-dominated magnetosphere of Saturn, hot plasma blobs rotate around the planet as observed in Figure 1e-h, resulting in the rotation of the auroral spiral. In addition to the corotation electric field, the motion of the energized plasma around Saturn is also driven by gradient and curvature drifts of the ions, which depend on the energy and, more importantly, on the L-shell. Due to this L-shell dependence, and despite the decrease of the corotation electric field drift with radial distance, the inner part of the hot plasma bubble drifts with a lower rate than its outer part, leading to an expansion of the energized plasma bubble as it rotates around Saturn [*Paranicas et al.*, 2007; *Brandt et al.*, 2008; *Müller et al.*, 2010], as observed in Figure 1e-h. While the plasma bubble expands, the auroral spiral winds with an increasing overlap. We should recall that ENA emissions appear only where charge exchange rates are high enough, so a direct correspondence between the ENA blob structure and the UV spiral arms is not expected. The limited ENA imaging resolution may also hide a fine structure in the ENA cloud.

4 Recurrence of the auroral spiral and the energized plasma

Extensive monitoring of ENA and aurora emissions between days 229 and 231 of 2016, allows the tracking of possible spiral and plasma energization before and after the observations shown in Figure 1. Selected observations are displayed in Figure 3.

INCA provided continuous observations of the ENA emissions between 12:04 on day 230 and 00:35 the day after. As described in Section 2.2, a clear signature of a plasma energization process, captured close to dusk at 17:29 (Figure 1e), intensified and rotated around Saturn towards the dayside. Earlier on day 230, at 12:23 (Figure 3j), ENA emissions were locally enhanced around 8-9 LT. This ENA cloud moved out of the INCA field of view during the following hours, preventing its accurate tracking. However, the emissions in the noon-to-dusk quadrant remained weak and diffuse throughout all the observations. At 14:24, UVIS data reveal a broad emission on the dayside, connecting two arcs of the main emission located at slightly different latitudes (Figure 3b). This could be considered as a spiral but not as clear as the one of Figure 1. Two hours later (Figure 3c), the aurora is still patchy but it is more structured showing two distinct emission layers, one equatorward to the other. This is seen as the beginning of a well-defined spiral morphology, with a distinct gap between the two emission curtains that appears fully developed 1 hr 25 mins later (Figure 1a).

Interestingly, if the plasma population responsible for the ENA cloud at 12:23 (Figure 3j) was subrotating around Saturn at 75% of full corotation, as is the case after 17:29 (Figure 2), it would have reached the dusk sector at ∼17:40, which is the time where the plasma energization was first observed. Therefore, the ENA cloud observed at 12:23 could be the result of plasma energization on the nightside, subrotating at ∼75% of rigid corotation, and becoming less intense in the postdawn sector. The absence of a significant local pressure enhancement in the magnetodisc at 14:24 can provide an explanation for the poorly defined spiral at that time. Later on, the same plasma population would be heated again after passing the dusk sector as shown in Figure 1.

The rotation of heated plasma was also observed on day 229 of 2016, as shown in Figure 3f-i. The observations start at 13:00 (Figure 3f) and reveal a hot plasma population in the postmidnight sector. This plasma bubble rotates, weakens on the dayside and becomes energized again after dusk (after 20:48), in the same local time sector as observed on day 230 after 17:29 (Figure 1). The population returns to the postmidnight sector at 01:00 (Figure 3i), ∼12 h after the start of the sequence, corresponding to 90% of corotation.

On day 229, UVIS scanned the northern auroral region 18 times between 17:52 and 22:41. One of those scans is displayed in Figure 3a. Despite the observed discontinuities in the aurora emission, a spiral-like structure is again present. However, contrary to the spiral observed one day later, the poleward part of the aurora seems to deviate from the

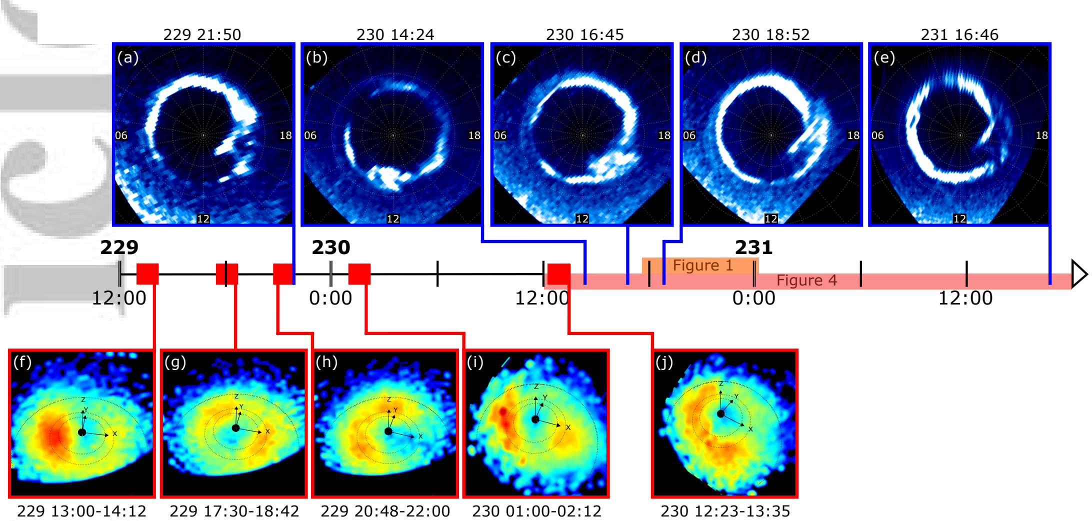

Figure 3. Timeline with Cassini/UVIS observations of Saturn's northern aurora (top) and Cassini/INCA ENA emission images (bottom) between day 229 of 2016 at 12:00 and day 231 at 18:00. Auroral and ENA observations are presented similarly to Figure 1. The time intervals covered by Figure 1 and Figure 4 are also indicated.

main emission in the post-noon sector, moving polewards and significantly lagging behind corotation (~45% of v_{cor}). This behavior appears to be consistent with the characteristics of an auroral bifurcation [*Radioti et al.*, 2011].

A few auroral scans were also acquired on day 231. The first scan at 16:46 (Figure 3e) reveals an auroral morphology similar to the one observed in the image acquired at 18:52 the day before (Figure 3d). The two images are separated by approximately 22 h, which roughly corresponds to two planetary rotations. This suggests that the nearly-corotating auroral spiral may have persisted over that period. The spiral structure can be nonetheless less defined on the dayside since its source plasma population is probably not energized enough to produce a clear spiral, as explained earlier. The ENA emissions on day 229 show that the plasma population can be energized again on the nightside at each planetary rotation so that this plasma pressure enhancement in the ring current could persist during several planetary rotations. This is also supported by the long-term thermal and hot plasma measurement analysis by *Sergis et al.* [2017]. Unfortunately, no ENA imaging was performed on day 231, preventing a confirmation of the presence of such a plasma blob in the inner magnetosphere.

Nevertheless, the Cassini in-situ measurements exhibit interesting features. While collecting the ENA, the INCA instrument applies a strong electric field created by high-voltage plates in the collimator and deflecting the charged particles. The high-voltage can be turned off, switching INCA to its ion operating mode detecting hydrogen and oxygen ions with energies between ~5 and 500 keV. At the start of day 231, INCA started to operate in ion mode until 13:00 when it switched back to neutral mode. The hydrogen ion intensities measured by INCA from 12:00 on day 230 to 18:00 on day 231 are shown in Figure 4a. Even in neutral mode, INCA's high energy channels still measure ions (mostly protons) that are not repelled by the collimator. At around 15:00 on day 230 (first arrow in Figure 4a), ions with energy exceeding 55 keV appear enhanced. Unlike ENAs, these ions do not move along a straight line so that the region where they originate cannot be determined. However, since they are detected at 8.8 LT, the energized ions are likely the in-situ counterpart of the ENA cloud visible in Figure 3j.

A second flux peak is observed at all energies at ~01:00 on day 231 when the instrument was switched back to ion mode. The particle intensities at energies >90 keV started to increase before the neutral to ion switch and subsequently dropped back to low values, suggesting that the peak is not due to the mode switching. The second peak is observed at 10 LT, which is the sector where the leading edge of the ENA cloud and the auroral spiral are expected to be located at ~01:00, i.e. ~1h after the end of the observations displayed in Figure 1.

Finally, the particle intensities in Figure 4a are significantly enhanced at ~11:30. This can be interpreted again as a signature of a hot plasma population rotating around Saturn but it cannot be confirmed because of the absence of simultaneous ENA images. However, this assumption is supported by the observation of the auroral spiral five hours later with the overlap in the dusk sector (Figure 3e). Recurrent structures also appear in the magnetic field measurements (Figure 4b-d) and will be discussed further below.

5 Discussion

We presented here a set of remote-sensing observations acquired with the Cassini spacecraft which sheds new light on the spiral morphology occasionally exhibited by Saturn's aurora. The UVIS auroral data together with the INCA observations of ENA emissions reveal that the spiral overlap region maps to a rotating localized enhancement of the

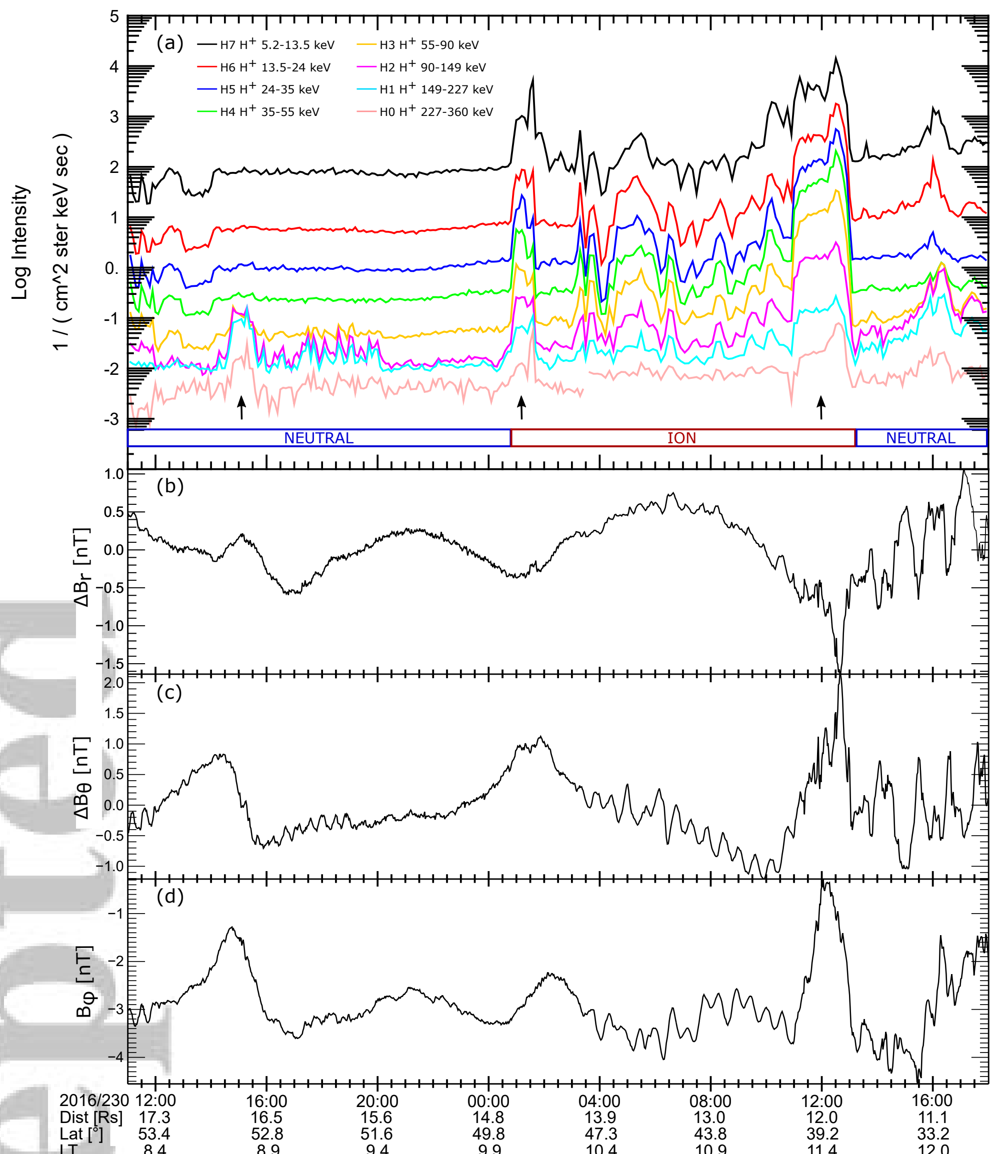

Figure 4. Magnetic field and Cassini/INCA proton measurements between 11:00 UT on day 230 of 2016 and 18:00 UT on day 231. The operating mode of the INCA instrument is indicated at the bottom of panel (a). Black arrows point to the flux enhancements discussed in the text. A third degree polynomial fit has been removed from the radial and polar components of the field.

magnetodisc plasma energy. The induced pressure gradients lead to a local time overlap of field-aligned currents producing the auroral spiral. The auroral spiral, which is rotating at ~85% of rigid corotation around the pole, is observed during two consecutive days, indicating that the magnetodisc plasma was re-energized several times during a few planetary rotations.

The hot plasma blob weakens after passing the dawn sector due to charge exchange losses and escape from the magnetosphere through the magnetopause. This intensity decrease might explain why an auroral spiral has never been identified with the LT overlap located close to noon: the pressure gradients are generally too small to create double layers of upward field-aligned currents in that region. In addition to the pressure gradient, the FAC density depends also on the gradient of the flux tube volume per unit magnetic flux (∇V in Equation 1) which is smaller on the dayside compared to the nightside where the field lines are stretched. Hence both factors ∇V and ∇p in Equation 1 do not favor the presence of a well-structured spiral in the noon local time sector. A re-energization of the plasma is required in the dusk sector to recover a clear spiral shape.

Observations of an auroral spiral have been rarely reported and the long spiral observation described here is unique. This rarity suggests that some particular conditions are required for the development of a long-standing auroral spiral. The energy of the plasma bubble in the magnetodisc has to be high enough to obtain large pressure gradients. After one rotation around Saturn, the re-energization might have to occur in phase with the crossing of the remnant of the former bubble to reach a sufficient energy.

Recurrent acceleration of plasma at every Saturn's rotation has already been identified by *Mitchell et al.* [2009], based on ENA, aurora and Saturn Kilometric Radiation observations. They located the acceleration region in the midnight-to-dawn quadrant. During the observations presented here, the plasma energization was initiated in the pre-midnight sector, intensified after midnight and recurred at a period close to Saturn's rotation period, as shown by the three proton flux peaks in Figure 4a, similarly to the period inferred by *Mitchell et al.* [2009] and *Rymer et al.* [2013]. *Mitchell et al.* [2009] associated the recurrent ring current enhancements with current sheet reconnection in the magnetotail driven by plasma mass loading. Moreover, continuous heating is associated with the transition between the thick current sheet on the dayside and the thin current sheet on the nightside [*Dialynas et al.*, 2013]. As they rotate from dusk to midnight, the flux tubes expand before being squeezed towards dawn. This process leads to pitch angle anisotropy, providing free energy for plasma waves. These waves would interact with charged particles to energize them and scatter them during each rotation.

Corotating pressure enhancement in the ring current (also referred to as partial ring current), due to periodic injections of energetic particles, drives currents which cause depressions of the magnetic field [*Khurana et al.*, 2009; *Brandt et al.*, 2010]. During the interval described here, the magnetic field is dominated by the radial component which shows similar periodic depressions (Figure 4b). *Brandt et al.* [2010] indicate that the field-aligned currents associated with the partial ring current would rotate together with the high pressure region. The magnetic field exhibits modulations at a period of just under 11 hours, which then might correspond with the period of northern planetary period oscillation (PPO) system (e.g. *Carbary and Mitchell* [2013]; *Hunt et al.* [2015]; *Provan et al.* [2019]). The magnetic perturbations are in phase with expectations based on the empirical PPO phase model by *Provan et al.* [2019]. PPOs also modulate the thickness of the current sheet [*Morooka et al.*, 2009; *Arridge et al.*, 2011; *Thomsen et al.*, 2017] and the radial displacements in the equatorial magnetospheric plasma [*Clarke et al.*, 2010]. A thin plasma sheet with outward plasma motions being more unstable, magnetic reconnection and plasmoid formation in Saturn's magnetotail are modulated by PPO [*Jackman et al.*, 2016; *Bradley et al.*, 2018], which could then explain the recurrent plasma energization at each planetary rotation.

In addition, the magnetic fluctuations are also typical of a magnetic dipolarization site crossing the spacecraft once every rotation (e.g. *Yao et al.* [2017a,c, 2018]). Magnetic dipolarization involves the formation of field-aligned currents and change of the magnetic geometry which will lead to an azimuthal motion of the dipolarization footpoint in the ionosphere, as explained by *Yao et al.* [2018]. As a consequence, an auroral intensification associated with a corotating dipolarized region would slightly subcorotate, as observed here.

6 Summary

Previous observations of Saturn's aurora have revealed that the main emission can occasionally exhibit a spiral structure. We presented here the first continuous observation of an auroral spiral over several hours. The spiral morphology stems from the presence of a localized hot plasma population in the magnetodisc which, due to pressure gradients at its boundaries, generates an additional layer of field-aligned currents in the current system associated with the main emission. The heated plasma is in rotation around Saturn and is re-energized in the nightside during several planetary rotations resulting in a long-standing auroral spiral. This study illustrates the importance of rotating magnetosphere-ionosphere coupling current system at Saturn and the perturbation on this current system induced by magnetospheric plasma inhomogeneities.

Acknowledgments

B.P., D.G. and J.C.G. are supported by the PRODEX program managed by ESA in collaboration with the Belgian Federal Science Policy Office. R.L.G. is supported by the Incoming Post-Docs in Sciences, Technology, Engineering, Materials and Agrobiotechnology (IPD-STEMA) project. Work at JHU/APL was supported by NASA under contracts NAS5-97271 and NNX07AJ69G and by subcontracts at the Office of Space Research and Technology of the Academy of Athens. The Cassini datasets used in this study are available through the Planetary Data System: UVIS data from https://atmos.nmsu.edu/pdsd/archive/data/co-s-uvis-2-cube-v14/couvis_0056/DATA, MIMI/INCA data from https://pds-ppi.igpp.ucla.edu/search/view/?f=null&id=pds://PPI/CO-S-MIMI-4-INCA-CALIB-V1.0/BROWSE/IENAMV0_SH7/2016, and MAG data from https://pds-ppi.igpp.ucla.edu/search/view/?f=null&id=pds://PPI/CO-E_SW_J_S-MAG-4-SUMM-1MINAVG-V2.0/DATA/2016.

References

Arridge, C. S., N. André, K. K. Khurana, C. T. Russell, S. W. H. Cowley, G. Provan, D. J. Andrews, C. M. Jackman, A. J. Coates, E. C. Sittler, M. K. Dougherty, and D. T. Young (2011), Periodic motion of Saturn's nightside plasma sheet, *Journal of Geophysical Research: Space Physics*, *116*, A11,205, doi:10.1029/2011ja016827.

Badman, S. V., E. J. Bunce, J. T. Clarke, S. W. H. Cowley, J.-C. Gérard, D. Grodent, and S. E. Milan (2005), Open flux estimates in Saturn's magnetosphere during the January 2004 Cassini-HST campaign, and implications for reconnection rates, *Journal of Geophysical Research*, *110*, A11,216, doi:10.1029/2005ja011240.

Badman, S. V., A. Masters, H. Hasegawa, M. Fujimoto, A. Radioti, D. Grodent, N. Sergis, M. K. Dougherty, and A. J. Coates (2013), Bursty magnetic reconnection at Saturn's magnetopause, *Geophysical Research Letters*, *40*, 1027–1031, doi:10.1002/grl.50199.

Bradley, T. J., S. W. H. Cowley, E. J. Bunce, A. W. Smith, C. M. Jackman, and G. Provan (2018), Planetary period modulation of reconnection bursts in Saturn's magnetotail, *Journal of Geophysical Research: Space Physics*, *123*, 9476–9507, doi: 10.1029/2018ja025932.

Brandt, P. C., J. Goldstein, B. J. Anderson, H. Korth, T. J. Immel, E. C. Roelof, R. DeMajistre, D. G. Mitchell, and B. Sandel (2005), On the relation between electric fields in the inner magnetosphere, ring current, auroral conductance, and plasmapause motion, in *Inner Magnetosphere Interactions: New Perspectives From Imaging*, pp. 159–166, American Geophysical Union, doi:10.1029/159gm12.

Brandt, P. C., C. P. Paranicas, J. F. Carbary, D. G. Mitchell, B. H. Mauk, and S. M. Krimigis (2008), Understanding the global evolution of Saturn's ring current, *Geophysical Research Letters*, *35*, L17,101, doi:10.1029/2008gl034969.

Brandt, P. C., K. K. Khurana, D. G. Mitchell, N. Sergis, K. Dialynas, J. F. Carbary, E. C. Roelof, C. P. Paranicas, S. M. Krimigis, and B. H. Mauk (2010), Saturn's periodic magnetic field perturbations caused by a rotating partial ring current, *Geophysical Research Letters*, *37*, L22,103, doi:10.1029/2010gl045285.

Bunce, E. J., S. W. H. Cowley, I. I. Alexeev, C. S. Arridge, M. K. Dougherty, J. D. Nichols, and C. T. Russell (2007), Cassini observations of the variation of Saturn's ring current parameters with system size, *Journal of Geophysical Research: Space Physics*, *112*, A10,202, doi:10.1029/2007ja012275.

Carbary, J. F., and D. G. Mitchell (2013), Periodicities in Saturn's magnetosphere, *Reviews of Geophysics*, *51*, 1–30, doi:10.1002/rog.20006.

Carbary, J. F., D. G. Mitchell, P. Brandt, E. C. Roelof, and S. M. Krimigis (2008), Track analysis of energetic neutral atom blobs at Saturn, *Journal of Geophysical Research: Space Physics*, *113*, A01,209, doi:10.1029/2007ja012708.

Clarke, K. E., D. J. Andrews, C. S. Arridge, A. J. Coates, and S. W. H. Cowley (2010), Magnetopause oscillations near the planetary period at Saturn: Occurrence, phase, and amplitude, *Journal of Geophysical Research: Space Physics*, *115*, A08,209, doi: 10.1029/2009ja014745.

Cowley, S. W. H., S. V. Badman, E. J. Bunce, J. T. Clarke, J.-C. Gérard, D. Grodent, C. M. Jackman, S. E. Milan, and T. K. Yeoman (2005), Reconnection in a rotation-dominated magnetosphere and its relation to Saturn's auroral dynamics, *Journal of Geophysical Research*, *110*, A02,201, doi:10.1029/2004ja010796.

Dialynas, K., P. C. Brandt, S. M. Krimigis, D. G. Mitchell, D. C. Hamilton, N. Krupp, and A. M. Rymer (2013), The extended Saturnian neutral cloud as revealed by global ENA simulations using Cassini/MIMI measurements, *Journal of Geophysical Research: Space Physics*, *118*(6), 3027–3041, doi:10.1002/jgra.50295.

Dialynas, K., E. Roussos, L. Regoli, C. P. Paranicas, S. M. Krimigis, M. Kane, D. G. Mitchell, D. C. Hamilton, N. Krupp, and J. F. Carbary (2018), Energetic ion moments and polytropic index in Saturn's magnetosphere using Cassini/MIMI measurements: A simple model based on κ-distribution functions, *Journal of Geophysical Research: Space Physics*, *123*, 8066–8086, doi:10.1029/2018ja025820.

Dougherty, M. K., H. Cao, K. K. Khurana, G. J. Hunt, G. Provan, S. Kellock, M. E. Burton, T. A. Burk, E. J. Bunce, S. W. H. Cowley, M. G. Kivelson, C. T. Russell, and D. J. Southwood (2018), Saturn's magnetic field revealed by the Cassini Grand Finale, *Science*, *362*, eaat5434, doi:10.1126/science.aat5434.

Esposito, L. W., C. A. Barth, J. E. Colwell, and et al. (2004), The Cassini Ultraviolet Imaging Spectrograph Investigation, *Space Science Review*, *115*, 299–361, doi:10.1007/s11214-004-1455-8.

Gérard, J.-C., D. Grodent, J. Gustin, A. Saglam, J. T. Clarke, and J. T. Trauger (2004), Characteristics of Saturn's FUV aurora observed with the Space Telescope Imaging Spectrograph, *Journal of Geophysical Research*, *109*, A09,207, doi:10.1029/2004JA010513.

Gérard, J.-C., B. Bonfond, J. Gustin, D. Grodent, J. T. Clarke, D. Bisikalo, and V. Shematovich (2009), Altitude of Saturn's aurora and its implications for the characteristic energy of precipitated electrons, *Geophysical Research Letters*, *36*, L02,202, doi:10.1029/2008GL036554.

Grodent, D. (2015), A Brief Review of Ultraviolet Auroral Emissions on Giant Planets, *Space Science Reviews*, *187*(1), 23–50, doi:10.1007/s11214-014-0052-8.

Grodent, D., J.-C. Gérard, S. W. H. Cowley, E. J. Bunce, and J. T. Clarke (2005), Variable morphology of Saturn's southern ultraviolet aurora, *Journal of Geophysical Research*, *110*, A07,215, doi:10.1029/2004JA010983.

Grodent, D., J. Gustin, J.-C. Gérard, A. Radioti, B. Bonfond, and W. R. Pryor (2011), Small-scale structures in Saturn's ultraviolet aurora, *Journal of Geophysical Research*, *116*, A09,225, doi:10.1029/2011JA016818.

Hunt, G. J., S. W. H. Cowley, G. Provan, E. J. Bunce, I. I. Alexeev, E. S. Belenkaya, V. V. Kalegaev, M. K. Dougherty, and A. J. Coates (2015), Field-aligned currents in Saturn's northern nightside magnetosphere: Evidence for interhemispheric current flow associated with planetary period oscillations, *Journal of Geophysical Research: Space Physics*, *120*, 7552–7584, doi:10.1002/2015ja021454.

Iijima, T., and T. A. Potemra (1978), Large-scale characteristics of field-aligned currents associated with substorms, *Journal of Geophysical Research*, *83*(A2), 599–615, doi: 10.1029/ja083ia02p00599.

Jackman, C. M., G. Provan, and S. W. H. Cowley (2016), Reconnection events in Saturn's magnetotail: Dependence of plasmoid occurrence on planetary period oscillation phase, *Journal of Geophysical Research: Space Physics*, *121*, 2922–2934, doi: 10.1002/2015ja021985.

Kane, M., D. G. Mitchell, J. F. Carbary, K. Dialynas, M. E. Hill, and S. M. Krimigis (2020), Convection in the magnetosphere of Saturn during the Cassini mission derived from MIMI INCA and CHEMS measurements, *Journal of Geophysical Research: Space Physics*, *125*(2), doi:10.1029/2019ja027534.

Khurana, K. K., D. G. Mitchell, C. S. Arridge, M. K. Dougherty, C. T. Russell, C. Paranicas, N. Krupp, and A. J. Coates (2009), Sources of rotational signals in Saturn's magnetosphere, *Journal of Geophysical Research: Space Physics*, *114*, A02,211, doi: 10.1029/2008ja013312.

Krimigis, S. M., D. G. Mitchell, D. C. Hamilton, and et al. (2004), Magnetosphere Imaging Instrument (MIMI) on the Cassini Mission to Saturn/Titan, *Space Science Review*, *114*, 233–329, doi:10.1007/s11214-004-1410-8.

Krimigis, S. M., N. Sergis, D. G. Mitchell, D. C. Hamilton, and N. Krupp (2007), A dynamic, rotating ring current around Saturn, *Nature*, *450*, 1050–1053, doi: 10.1038/nature06425.

Lamy, L., R. Prangé, W. Pryor, J. Gustin, S. V. Badman, H. Melin, T. Stallard, D. G. Mitchell, and P. C. Brandt (2013), Multispectral simultaneous diagnosis of Saturn's aurorae throughout a planetary rotation, *Journal of Geophysical Research: Space Physics*, *118*, 4817–4843, doi:10.1002/jgra.50404.

Lamy, L., R. Prangé, C. Tao, T. Kim, S. V. Badman, P. Zarka, B. Cecconi, W. S. Kurth, W. Pryor, E. Bunce, and A. Radioti (2018), Saturn's northern aurorae at solstice from HST observations coordinated with Cassini's Grand Finale, *Geophysical Research Let-*

ters, *45*, 9353–9362, doi:10.1029/2018GL078211.

Meredith, C. J., S. W. H. Cowley, and J. D. Nichols (2014), Survey of Saturn auroral storms observed by the Hubble Space Telescope: Implications for storm time scales, *Journal of Geophysical Research: Space Physics*, *119*, 9624–9642, doi: 10.1002/2014ja020601.

Mitchell, D., S. Krimigis, C. Paranicas, and et al. (2009), Recurrent energization of plasma in the midnight-to-dawn quadrant of Saturn's magnetosphere, and its relationship to auroral UV and radio emissions, *Planetary and Space Science*, *57*, 1732–1742, doi:10.1016/j.pss.2009.04.002.

Mitchell, D. G., P. C. Brandt, E. C. Roelof, and et al. (2005), Energetic ion acceleration in Saturn's magnetotail: Substorms at Saturn?, *Geophysical Research Letters*, *32*, L20S01, doi:10.1029/2005gl022647.

Mitchell, D. G., P. C. Brandt, J. H. Westlake, S. E. Jaskulek, G. B. Andrews, and K. S. Nelson (2016), Energetic particle imaging: The evolution of techniques in imaging high-energy neutral atom emissions, *Journal of Geophysical Research: Space Physics*, *121*(9), 8804–8820, doi:10.1002/2016ja022586.

Morooka, M. W., R. Modolo, J.-E. Wahlund, M. André, A. I. Eriksson, A. M. Persoon, D. A. Gurnett, W. S. Kurth, A. J. Coates, G. R. Lewis, K. K. Khurana, and M. Dougherty (2009), The electron density of Saturn's magnetosphere, *Annales Geophysicae*, *27*, 2971–2991, doi:10.5194/angeo-27-2971-2009.

Müller, A. L., J. Saur, N. Krupp, E. Roussos, B. H. Mauk, A. M. Rymer, D. G. Mitchell, and S. M. Krimigis (2010), Azimuthal plasma flow in the Kronian magnetosphere, *Journal of Geophysical Research*, *115*, A08,203, doi:10.1029/2009ja015122.

Nichols, J. D., S. V.Badman, K. H. Baines, and et al. (2014), Dynamic auroral storms on Saturn as observed by the Hubble Space Telescope, *Geophysical Research Letters*, *41*, 3323–3330, doi:10.1002/2014gl060186.

Palmaerts, B., A. Radioti, D. Grodent, Z. H. Yao, T. J. Bradley, E. Roussos, L. Lamy, E. J. Bunce, S. W. H. Cowley, N. Krupp, W. S. Kurth, J.-C. Gérard, and W. R. Pryor (2018), Auroral storm and polar arcs at Saturn - Final Cassini/UVIS auroral observations, *Geophysical Research Letters*, *45*, 6832–6842, doi:10.1029/2018gl078094.

Paranicas, C., D. G. Mitchell, E. C. Roelof, B. H. Mauk, S. M. Krimigis, P. C. Brandt, M. Kusterer, F. S. Turner, J. Vandegriff, and N. Krupp (2007), Energetic electrons injected into Saturn's neutral gas cloud, *Geophysical Research Letters*, *34*(2), doi:

10.1029/2006gl028676.

Provan, G., L. Lamy, S. W. H. Cowley, and E. J. Bunce (2019), Planetary Period Oscillations in Saturn's magnetosphere: Comparison of magnetic and SKR modulation periods and phases during northern summer to the end of the Cassini mission, *Journal of Geophysical Research: Space Physics*, *124*, 1157–1172, doi:10.1029/2018ja026079.

Radioti, A., D. Grodent, J.-C. Gérard, S. E. Milan, B. Bonfond, J. Gustin, and W. Pryor (2011), Bifurcations of the main auroral ring at Saturn: Ionospheric signatures of consecutive reconnection events at the magnetopause, *Journal of Geophysical Research*, *116*, A11,209, doi:10.1029/2011JA016661.

Radioti, A., E. Roussos, D. Grodent, J.-C. Gérard, N. Krupp, D. G. Mitchell, J. Gustin, B. Bonfond, and W. Pryor (2013), Signatures of magnetospheric injections in Saturn's aurora, *Journal of Geophysical Research: Space Physics*, *118*, 1922–1933, doi: 10.1002/jgra.50161.

Radioti, A., D. Grodent, J.-C. Gérard, E. Roussos, D. Mitchell, B. Bonfond, and W. Pryor (2015), Auroral spirals at Saturn, *Journal of Geophysical Research: Space Physics*, *120*, 8633–8643, doi:10.1002/2015ja021442.

Radioti, A., D. Grodent, X. Jia, J.-C. Gérard, B. Bonfond, W. Pryor, J. Gustin, D. Mitchell, and C. Jackman (2016), A multi-scale magnetotail reconnection event at Saturn and associated flows: Cassini/UVIS observations, *Icarus*, *263*, 75–82, doi: 10.1016/j.icarus.2014.12.016.

Radioti, A., Z. Yao, D. Grodent, B. Palmaerts, E. Roussos, K. Dialynas, D. Mitchell, Z. Pu, S. V. Badman, J.-C. Gérard, W. Pryor, and B. Bonfond (2019), Auroral beads at Saturn and the driving mechanism: Cassini proximal orbits, *The Astrophysical Journal Letters*, *885*, L16, doi:10.3847/2041-8213/ab4e20.

Sergis, N., C. M. Jackman, M. F. Thomsen, S. M. Krimigis, D. G. Mitchell, D. C. Hamilton, M. K. Dougherty, N. Krupp, and R. J. Wilson (2017), Radial and local time structure of the Saturnian ring current, revealed by Cassini, *Journal of Geophysical Research: Space Physics*, *122*, 1803–1815, doi:10.1002/2016ja023742.

Rymer, A. M., D. G. Mitchell, T. W. Hill, E. A. Kronberg, N. Krupp, and C. M. Jackman (2013), Saturn's magnetospheric refresh rate, *Geophysical Research Letters*, *40*, 2479–2483, doi:10.1002/grl.50530.

Sergis, N., E. J. Bunce, J. F. Carbary, S. W. H. Cowley, X. Jia, D. C. Hamilton, S. M. Krimigis, D. G. Mitchell, and M. K. Dougherty (2018), The Ring Current of Saturn, in *Electric Currents in Geospace and Beyond*, pp. 139–154, John Wiley & Sons, Inc., doi:10.1002/9781119324522.ch9.

Thomsen, M. F., C. M. Jackman, S. W. H. Cowley, X. Jia, M. G. Kivelson, and G. Provan (2017), Evidence for periodic variations in the thickness of Saturn's nightside plasma sheet, *Journal of Geophysical Research: Space Physics*, *122*(1), 280–292, doi: 10.1002/2016ja023368.

Vasyliunas, V. M. (1970), Mathematical Models of Magnetospheric Convection and its Coupling to the Ionosphere, in *Particles and Fields in the Magnetosphere*, vol. 17, edited by B. M. McCormac, pp. 60–71, Springer Netherlands, doi:10.1007/978-94-010-3284-1_6.

Wilson, R. J., F. Bagenal, and A. M. Persoon (2017), Survey of thermal plasma ions in saturn's magnetosphere utilizing a forward model, *Journal of Geophysical Research: Space Physics*, *122*(7), 7256–7278, doi:10.1002/2017ja024117.

Yao, Z. H., D. Grodent, L. C. Ray, I. J. Rae, A. J. Coates, Z. Y. Pu, A. T. Lui, A. Radioti, J. H. Waite, G. H. Jones, R. L. Guo, and W. R. Dunn (2017a), Two fundamentally different drivers of dipolarizations at Saturn, *Journal of Geophysical Research: Space Physics*, *122*, 4348–4356, doi:10.1002/2017ja024060.

Yao, Z. H., A. J. Coates, L. C. Ray, I. J. Rae, D. Grodent, G. H. Jones, M. K. Dougherty, C. J. Owen, R. L. Guo, W. R. Dunn, A. Radioti, Z. Y. Pu, G. R. Lewis, J. H. Waite, and J.-C. Gérard (2017c), Corotating magnetic reconnection site in Saturn's magnetosphere, *The Astrophysical Journal Letters*, *846*, L25, doi:10.3847/2041-8213/aa88af.

Yao, Z. H., A. Radioti, D. Grodent, L. C. Ray, B. Palmaerts, N. Sergis, K. Dialynas, A. J. Coates, C. S. Arridge, E. Roussos, S. V. Badman, S.-Y. Ye, J.-C. Gérard, P. A. Delamere, R. L. Guo, Z. Y. Pu, J. H. Waite, N. Krupp, D. G. Mitchell, and M. K. Dougherty (2018), Recurrent magnetic dipolarization at Saturn: Revealed by Cassini, *Journal of Geophysical Research: Space Physics*, *123*, 8502–8517, doi: 10.1029/2018ja025837.

Zheng, Y., A. T. Lui, M.-C. Fok, B. J. Anderson, P. C. Brandt, and D. G. Mitchell (2008), Controlling factors of Region 2 field-aligned current and its relationship to the ring current: Model results, *Advances in Space Research*, *41*, 1234–1242, doi: 10.1016/j.asr.2007.05.084.